AIP Journal of Applied Physics

Fermi level spin polarization of polycrystalline thulium by point contact Andreev reflection spectroscopy

P. Stamenov and J. M. D. Coey

Citation: Journal of Applied Physics **109**, 07C713 (2011); doi: 10.1063/1.3554254
View online: http://dx.doi.org/10.1063/1.3554254
View Table of Contents: http://scitation.aip.org/content/aip/journal/jap/109/7?ver=pdfcov
Published by the AIP Publishing

Fermi level spin polarization of polycrystalline thulium by point contact Andreev reflection spectroscopy

P. Stamenov[a] and J. M. D. Coey
School of Physics and CRANN, Trinity College, Dublin 2, Ireland

(Presented 16 November 2010; received 24 September 2010; accepted 22 November 2010; published online 28 March 2011)

The spin polarization near the Fermi level in bulk polycrystalline ferrimagnetic thulium is investigated by means of point contact Andreev reflection (PCAR), in the temperature interval (1.9–9.2 K). The highest polarization measured is $P = 0.41(8)$, with barrier parameter $Z = 0.39(8)$, proximity region gap of $\Delta_1 = 1.26(5)$ meV and an elevation of the electronic temperature of $\Delta T_e = 3.3(8)$ K, for a lattice temperature of $T = 2.20(5)$ K, and a contact conductance of $G = 330(5)$ G_0. Both polarization and barrier power are found to be constant within the experimental uncertainties in the entire accessible temperature interval and linearly independent, while the proximity gap was found to obey the standard BCS temperature dependence with a $T_{cGap} = 10.2(2)$ K, higher than the $T_{cGap} = 9.2$ K of bulk niobium. Despite its low ordering temperature, thulium could be suitable candidate for low critical current spin-transfer-torque demonstrations. © *2011 American Institute of Physics*. [doi:10.1063/1.3554254]

Rare-earth elements exhibit complicated magnetic structures and rich magnetic phase diagrams. Their compounds could provide prototypes of low- or zero-net magnetic moment materials, with significant Fermi level spin polarization and large spin–orbit coupling features of interest for general spin-electronic applications and, in particular, for spin-transfer-torque-based devices. The light rare-earths are prone to oxidation, and corrosion and any exposed surfaces rapidly deteriorate when manipulated in ambient conditions. Thulium, as an example of the heavier rare-earths, is stable in the air, can be polished, and exhibits an interesting (↑↑↑↑, ↓↓↓, ↑↑↑↑, ↓↓↓, ...) *c*-axis ferrimagnetic ground state (below about 25 K), with a net moment of 0.75 μ_B/atom, as confirmed by neutron[1,2] and resonant x-ray[3] scattering and macroscopic magnetization.[4]

Here we present a PCAR spectroscopic study of polycrystalline thulium, focused on the determination of the Fermi level spin polarization, the temperature evolution of the superconducting proximity effect, as well as the stability and reliability of the extracted parameters. Spin polarization is an essential concept in spin-electronics and various working definitions exist,[5]

$$P^{[i]} = \frac{\langle D_\uparrow v_\uparrow^i \rangle - \langle D_\downarrow v_\downarrow^i \rangle}{\langle D_\uparrow v_\uparrow^i \rangle + \langle D_\downarrow v_\downarrow^i \rangle}. \quad (1)$$

where $D_\downarrow$ is the spin polarized density of states (in principle function of energy), $v_\downarrow$ is the electronic velocity or one of its components, and i can have values of 0, 1, or 2. The angle brackets in Eq. (1) denote averaging over energy and momentum and the nature of the averaging and the appropriate value of i does depend on the method of choice for the measurement of spin polarization.[5] Hereafter a value of $i = 2$ is assumed (i.e., close to diffusive electronic transport) to be applicable to the polarization determined by means of PCAR (Ref. 6).

The experiments are performed at temperatures from 1.9 to 10 K, with no externally applied magnetic field, in a He vapor flow cryostat (Oxford Instruments), equipped with a differential micrometer drive and a single-axis piezo positioner. The basics of the setup are similar to the ones described in reference (Ref. 7). A niobium shear-cut tip is used for the superconducting side of the point contacts. Low frequency ($f = 1.23$ kHz) voltage sourcing and current sensing is used in a conjunction with a DSP lock-in system (Perkin Elmer 7265 in conjunction with a Stanford Research SR570 low-noise current preamplifier) capable of recording data at a rate better than one Andreev spectrum per second. Averaging is performed when and if necessary, after the measurements.

A numerically efficient matrix implementation of a modified BTK (Ref. 8) theory, taking into account superconducting proximity, electronic heating, modulation broadening and series resistance, is used for least squares fitting of the experimental data. The algorithm is also based on the extensions by Mazin *et al.*[9] for the case diffusive transport, and the work of Woods *et al.*[10] on the ballistic and diffusive regimes. Fixed closed interval difference norm minimization is used, rather than guess value generalized gradient minimization, for its robustness and only marginally higher computational cost. $|\chi|$ is the norm of the difference between the data and model vectors. Typically reduced χ values reached are of the order of 10^{-5}. The data vectors contain a fixed number (usually between 200 and 1000) elements.

The treatment of the superconducting proximity effect is done following Stijkers *et al.*[11] through the introduction of two different effective gap energies—Δ_1 and Δ_2. The first one Δ_1 for the Andreev reflection process, and the second one Δ_2 for the quasiparticle transport. Δ_1 is a fitting parameter, while Δ_2 is typically fixed at the value for bulk superconducting

[a]Electronic mail: stamenov.plamen@tcd.ie.

Niobium ($\Delta_2 = 1.5$ meV, $T_c = 9.2$ K) and essentially serves as an applied bias reference for the investigated point contact, at temperatures $T < T_c$ for the superconducting tip, which is important for contacts with non-negligible series resistance contribution.

Thermal broadening is introduced using the derivative of the Fermi distribution function explicitly, and not through an effective "smearing" Gaussian,[12]

$$f(\epsilon, T) = -\{\exp[(\epsilon - \epsilon_F)/k_B T]/k_B T\} \times \{1 + \exp[(\epsilon - \epsilon_F)/k_B T]\}^{-2}, \quad (2)$$

where ϵ_F is the Fermi level and k_B is Boltzmann's constant. This is done using matrix convolution in a discreet voltage base for either the conductance or the differential conductance, resulting in a substantially faster algorithm than achievable through direct quadrature integration. Modulation broadening is also considered in a similar matrix approach, directly for the differential conductance, through the convolution function,

$$g(\epsilon, V_m) = (1/\pi q V_m)\left[1 - \left(\epsilon^2/q^2 V_m^2\right)\right]^{1/2}, \quad (3)$$

where V_m is the amplitude of the modulation voltage used and q is the absolute value of the elementary charge. However, its effect on the acquired data is experimentally limited by controlling the amplitude of the applied differentiation voltage.

When relatively high interfacial barriers are present at the point contact, the distribution of the injected quasiparticles can differ significantly from the equilibrium one (characterized by an electronic temperature $T_e = T$ equal to the lattice one). This is taken into account by introducing an additional fitting parameter ΔT_e, so that $T_e = T + \Delta T_e$. For very transparent contacts $\Delta T_e \to 0$.

Critical current artifacts[13] limit the bias window that can be utilized for measurements. For a typical point contact the useful bias window is on the order of $3\Delta_2 - 7\Delta_2$, depending primarily on the lateral size on the contact. The measured values of the polarization can also incorporate an additional contact size dependence,[14] arising from spin–orbit scattering, thus a large set of contacts is typically formed with the largest evaluated polarization P being taken as representative of the material under investigation. For a summary of the various imperfections observable in PCAR spectroscopy data, see the work of Baltz *et al.*[15]

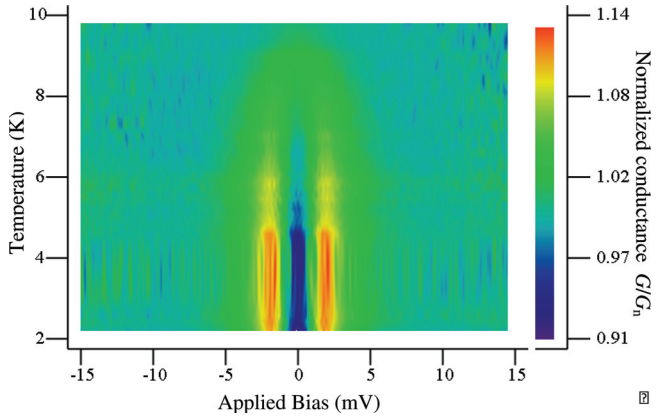

FIG. 2. (Color online) Temperature evolution of the normalized differential conductance for a Nb/Tm point contact.

Up to nine fitting parameters are used for each independent contact model (usually just one model) used. Four of them, corresponding to Δ_1, P, Z and ΔT_e, are used conventionally. Another five parameters are used to perform various equipment-associated artifacts, such as, small changes of the gains and offsets of the filtering amplifiers and series resistance contribution. The resulting fitting algorithm can be used for effective real-time interpretation of PCAR data. An example of a PCAR spectrum, obtained at a lattice temperature of $T = 2.2$ K, and representative of the highest polarization observed for thulium are shown in Fig. 1. The observed polarization $P = 0.41(9)$ is comparable to those found for the 3d elements (Fe, Co, and Ni),[6,16] despite the large value of the barrier parameter $Z = 0.39(8)$. At this relatively small contact size, with normal state conductance of $G_n = 35.5(5)G_0$, electronic heating is also non-negligible with $\Delta T_e = 3.3(8)$ K. Reasonable fits can only be obtained for values of the proximity gap substantially smaller than Δ_2, namely $\Delta_1 = 1.26(5)$ meV.

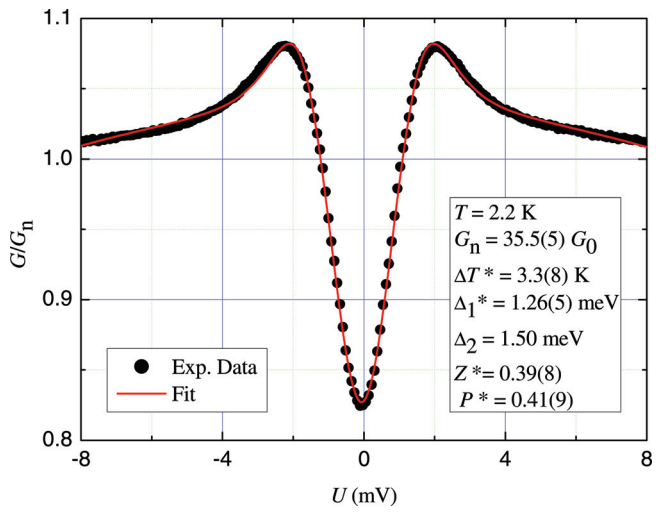

FIG. 1. (Color online) Modified BTK theory fit to the normalized differential conductance of a Nb/Tm point contact. (*) designates the fitted parameters.

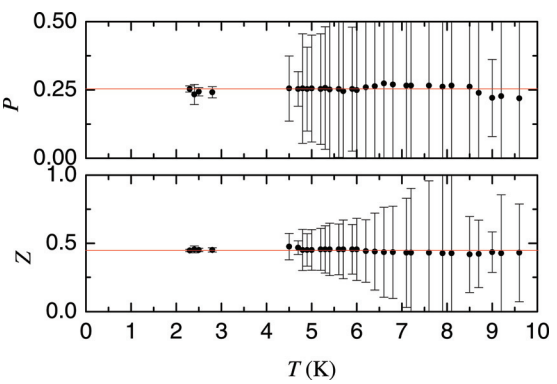

FIG. 3. (Color online) Temperature dependencies of the polarization P and the barrier parameter Z. The lines are guides to the eye.

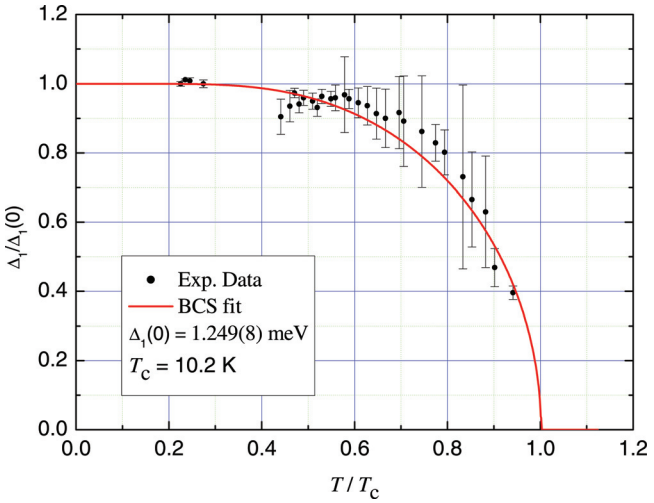

FIG. 4. (Color online) Temperature dependence of the normalized gap for the superconducting proximity region.

To further characterize the contacts, temperature can be varied while keeping the contact size constant. Such a dependence is visualized in Fig. 2, for a different contact formed on the same surface. The shifting of the positive differential conductance peaks toward zero bias with the increasing temperature is primarily due to the temperature variation of the proximity gap $\Delta_1(T)$, which will be investigated, in more detail, further below. The systematic drop of peak differential conductance amplitudes is due to the "averaging" effect of the thermal broadening, and little structure is observed in the spectra taken above the T_c of the bulk of the Niobium tip.

The above temperature effects can be further analyzed by fitting the individual differential conductance spectra comprising Fig. 2. The resulting temperature dependencies of the polarization $P(T)$ and the barrier parameter $Z(T)$ are shown in Fig. 3. Remarkably, both P and Z are essentially constant as functions of temperature in the entire accessible interval. This confirms the reliability of the extracted parameters, despite the diverging statistical uncertainties, even in the region $T \sim T_c$, where the method of calculating the statistical fitting errors (using Jacobian and covariance matrices, which depend on the smallness of the relative uncertainties) fails completely. This stability is not guaranteed *a priori*. It is a result of the sufficiently different values of Δ_1 and Δ_2, which yield linearly independent values of P and Z. This is unlike the usual procedure, which consists of extrapolating the weak parabolic dependence $P(Z)$ toward $Z \rightarrow 0$, as, for example in the work of Strijkers *et al.*[11]

Even more intriguing is the temperature dependence of Δ_1, visualized in Fig. 4. The simplest expectation is that $\Delta_1(T)$ would follow, or decay even more abruptly than $\Delta_2(T)$. However, assuming that the normalized superconducting gap would follow the standard BCS (Ref. 17) dependence $\Delta(T/T_c)/\Delta(0)$, the fit (shown on Fig. 4) results in a value for $T_c = 10.2$ K, which is higher than the one for bulk Niobium (9.2 K). This implies that either Δ_2 is affected by the enhanced spin–orbit coupling at the thulium/niobium interface, or that the $\Delta_1(T)$ does not obey the standard BCS dependence.

In conclusion, the Fermi level spin polarization of bulk thulium is determined to be constant, $P = 0.41(9)$, at temperatures below about 10 K. In view of this, and its low saturation magnetization of 0.75 μ_B/atom, thulium may be a good candidate material for spin-transfer-torque-based low-temperature demonstrations of memory or logic elements and oscillators.

ACKNOWLEDGMENTS

We acknowledge the support from SFI and EU within the SPINCURRENTS network.

[1]W. C. Koehler, J. W. Cable, E. O. Wollan, and M. K. Wilkinson, J. Appl. Phys. **33**, 1124 (1962).
[2]W. C. Koehler, J. W. Cable, E. O. Wollan, and M. K. Wilkinson, Phys. Rev. **126**, 1672 (1962).
[3]J. Bohr, D. Gibbs, and K. Huang, Phys. Rev. B **42**, 4322 (1990).
[4]D. B. Richards and S. Legvold, Phys. Rev. **186**, 508 (1969).
[5]I. I. Mazin, Phys. Rev. Lett. **83**, 1427 (1999).
[6]R. J. Soulen, J. M. Byers, M. S. Osofsky, B. Nadgorny, T. Ambrose, S. F. Cheng, P. R. Broussard, C. T. Tanaka, J. Nowak, J. S. Moodera, A. Barry, and J. M. D. Coey, Nature **282**, 85 (1998).
[7]R. J. Soulen, M. S. Osofsky, B. Nadgorny, T. Ambrose, P. Brous-sard, S. F. Cheng, J. Byers, C. T. Tanaka, J. Nowack, J. S. Moodera, G. Laprade, A. Barry, and M. D. Coey, J. Appl. Phys. **85**, 4589 (1999).
[8]G. E. Blonder, M. Tinkham, and T. M. Klapwijk, Phys. Rev. B **25**, 4515 (1982).
[9]I. I. Mazin, A. A. Golubov, and B. Nadgorny, J. Appl. Phys. **89**, 7576 (2001).
[10]G. T. Woods, R. J. Soulen, I. Mazin, B. Nadgorny, M. S. Osofsky, J. Sanders, H. Srikanth, W. F. Egelhoff, and R. Datla, Phys. Rev. B **70**, 154416 (2004).
[11]G. J. Strijkers, Y. Ji, F. Y. Yang, C. L. Chien, and J. M. Byer, Phys. Rev. B **63**, 104510 (2001).
[12]Y. Bugoslavsky, Y. Miyoshi, S. K. Clowes, W. R. Branford, M. Lake, I. Brown, A. D. Caplin, and L. F. Cohen, Phys. Rev. B **71**, 104523 (2005).
[13]G. Sheet, S. Mukhopadhyay, and P. Raychaudhuri, Phys. Rev. B **69**, 134507 (2004).
[14]M. Stokmaier, G. Goll, D. Weissenberger, C. Sürgers, and H. v. Löhneysen, Phys. Rev. Lett. **101**, 147005 (2008).
[15]V. Baltz, A. D. Naylor, K. M. Seemann, W. Elder, S. Sheen, K. Westerholt, H. Zabel, G. Burnell, C. H. Marrows, and B. J. Hickey, J. Phys.: Condens. Matter **21**, 095701 (2009).
[16]S. K. Upadhyay, A. Palanisami, R. N. Louie, and R. A. Buhrman, Phys. Rev. Lett. **81**, 3247 (1998).
[17]J. Bardeen, L. N. Cooper, and J. R. Schrieffer, Phys. Rev. **108**, 1175 (1957).